Lab on a Chip

PAPER

View Article Online
View Journal | View Issue

Cite this: *Lab Chip*, 2015, **15**, 1160

Creased hydrogels as active platforms for mechanical deformation of cultured cells†‡

Dayong Chen,[a] Robert D. Hyldahl§[b] and Ryan C. Hayward*[a]

Received 2nd November 2014,
Accepted 16th December 2014

DOI: 10.1039/c4lc01296h

www.rsc.org/loc

Cells cultured *in vitro* using traditional substrates often change their behavior due to the lack of mechanical deformation they would naturally experience *in vivo*. To mimic the *in vivo* mechanical environment, we design temperature-responsive hydrogels with patterned surface creases as dynamic cell stretching devices. A one-step photolithographic method is first employed to pattern integrin-binding peptides on the gel, causing single cells or several-cell clusters to adhere to the surface in registry with creases. A variety of crease patterns are prescribed on a single substrate, enabling the mechanical deformation of cultured myoblast cells with different strain states and achieving tensile strain as high as 0.2. As creases provide large amplitude local deformation of the gel surface without the need for macroscopic deformation, can be formed on gels covering a wide range of modulus, and can be actuated using a variety of stimuli, they hold the potential to enable the design of high throughput and versatile platforms for mechano-biological studies.

Introduction

Cells cultured *in vitro* using traditional substrates often change their behavior due to the lack of important cues that they would naturally experience *in vivo*.[1–16] One example is mechanical deformation, which is known to play an important role in the life cycle of cells by modulating behaviors including growth, differentiation, polarization, motility, contractility, and apoptosis (programmed cell death).[1–6] Such effects are of particular importance for muscle cells, which constantly experience mechanical deformation *in vivo* due to motion of the body, breathing, and operation of the cardiovascular system.[4,17,18] The processes by which mechanical deformations are converted into biochemical signals and integrated into cellular responses, *i.e.*, 'cellular mechanotransduction', involve numerous signaling molecules and cellular components such as ion-channel proteins, myosin motors, and cytoskeletal filaments.[19,20] Central roles are played by mechanical coupling between the extracellular matrix (ECM) and the cytoskeleton through transmembrane proteins known as integrins that localize into focal adhesions, and by intercellular adhesion *via* another type of transmembrane proteins called cadherins.[21,22] Many studies on cellular mechanotransduction have focused on modulating the stiffness and geometry of substrates, and tracking how cells sense and deform these substrates.[23–29] These approaches, however, only partially mimic the environment cells experience *in vivo*, where cells not only sense the stiffness and geometry of their surrounding tissues, but are also actively deformed by them. While the important influence of mechanical deformation on cell behavior is generally acknowledged,[1] efforts to characterize these effects, and to obtain a detailed understanding of the underlying mechanotransduction pathways, remain in their nascent stages. This is in part due to the difficulty of isolating the effects of mechanical deformation from the convoluted influence of other biochemical cues, which is in large part compounded by the lack of convenient experimental methods for applying well-controlled mechanical deformation to cultured cells in a high-throughput fashion.

Methods to mechanically strain cells have generally relied either on uniform macroscopic deformation of an elastic cell culture matrix/substrate (using devices such as those sold commercially by Flexcell International),[30,31] or on highly localized deformation of a portion of the cell using an AFM tip, a micropipette, optical tweezers or magnetically-loaded beads or posts.[22,32–36] The former set of techniques can be difficult to integrate with *in situ* methods to characterize cellular response, since any given material point undergoes displacements of order the macroscopic sample size.[30] While techniques based on microscopic deformation largely circumvent these limitations, they suffer from non-uniform and poorly

[a] *Department of Polymer Science and Engineering, University of Massachusetts, Amherst, MA 01003, USA. E-mail: rhayward@mail.pse.umass.edu; Fax: +1 413 545 0082; Tel: +1 413 577 1317*
[b] *Department of Kinesiology, University of Massachusetts, Amherst, MA 01003, USA*
† Dedicated to Professor Priscilla M. Clarkson (1947–2013)
‡ Electronic supplementary information (ESI) available. See DOI: 10.1039/c4lc01296h
§ Present address: Department of Exercise Sciences, Brigham Young University, Provo, UT 84602, USA.

characterized strain fields, and generally allow for deformation of only one cell at a time.[37] Another method to apply deformation to cultured cells is through shear flow of fluids, although this represents a physiologically relevant state only for a few specific types of cells.[38] Cells have also been put under hydrostatic compression using osmotic pressure, however, this loading state is primarily relevant only for processes of anhydrobiosis and apoptosis.[39]

Recently, an area of considerable interest has been the fabrication of micro-scale devices that can apply well-defined strains at the single- or multi-cell level, without requiring macroscopic deformation of the device. The ability to study the response of isolated cells and controlled clusters would be valuable for probing the role of intercellular interactions in mechano-biological responses. Parallel arrays of these devices could allow for the simultaneous application of a variety of different mechanical strains to cultured cells, thus allowing the systematic manipulation of multiple mechano-biological parameters and opening the door to high-throughput studies. Furthermore, such micro-scale devices would facilitate integration of mechanical deformation into the CO_2- and temperature-controlled, sterile, fluidic environments required for cell culture. While approaches based on Braille displays[31] and micromembranes[40–45] actuated by hydraulic/pneumatic pressure changes have been developed to stretch multiple cells with millimeter-scale deformations, we are aware of only one approach based on micro-fabricated dielectric elastomers that has the potential to operate at the single cell level.[46,47] However, the use of the device with cultured cells has yet to be demonstrated, due to its susceptibility to short circuiting, dielectric and electro-mechanical instabilities associated with dielectric elastomers.[46,47] Mechanically wrinkled substrates have also been studied as cell culture substrates;[13–16] to date, however, the emphasis of this work has been primarily to alter surface topography, rather than to mechanically deform cultured cells.

Here, we describe an approach to cell stretching devices that can operate at the level of single cells or small cell clusters, based on the creasing instability of hydrogel films. Using cultured myoblast cells, we demonstrate the application of strain amplitudes up to 0.20, with strain states varying from plane strain to equibiaxial tension on a single chip. Such single-chip devices are readily incorporated into cell culture environments and open the door to high throughput mechano-biological studies. Furthermore, the method makes use of soft hydrogel substrates that can be modulated to have a wide range of physiologically-relevant elastic moduli.

Materials and methods

Preparation of surface-attached hydrogels

Hydrogels are prepared from degassed aqueous pre-gel solutions containing 808.9 mM *N*-isopropylacrylamide (NIPAM), 80.6 mM sodium acrylate (NaAc), and 6.3 mM *N*,*N*′-methylenebisacrylamide (BisAA). For gels on substrates with parallel stripe patterns, to initiate free radical polymerization, 0.3 μL of *N*,*N*,*N*′,*N*′-tetramethylethylenediamine as catalyst and 1.0 μL of a 10 wt% aqueous ammonium persulfate solution as initiator are added to 200 μL of pre-gel solution. As shown in Fig. S4,† the mixture is loaded by capillary force between a substrate and a release coverslip separated by spacers (Kapton® 300HN films, DuPont) to define the thickness of the gel (H = 76 μm). Gelation is carried out for at least 30 min in a nitrogen-filled sealed chamber. For gels on substrates with elliptical and circular patterns, the pre-gel solution is mixed with 10 μL of 3 wt% aqueous solution of 2,2′-azobis[2-methyl-*N*-(2-hydroxyethyl)propionamide] (Wako Pure Chemical Industries, VA-086). The polymerization is initiated by applying 365 nm UV light (5 mW in power), allowing 20 min for the reaction to proceed. To covalently attach gels to substrates, glass substrates are pretreated with the [3-(methacryloxy)-propyl] trimethoxysilane–ethanol solution for at least 6 h. To characterize the cross-section of creased hydrogels using a laser scanning confocal fluorescence microscope (Zeiss), a small amount (3.2×10^{-5} mmol) of a Rhodamine B-labeled methacrylate is incorporated into the 200 μL pre-gel solution. Topographically patterned glass substrates are lithographically fabricated following a previous report.[48] Specifically, as illustrated in Fig. S4,† SU-8 molds with a thickness of 40 μm are photo-lithographically patterned, from which PDMS (Sylgard 184, Dow Corning, base: crosslinker in a 10 : 1 mixing ratio by weight) negative replicas are cast and fully cured at 70 °C for 12 h. Topographic patterns are then prepared using the PDMS mold with Norland optical adhesive (Norland 81), cured with 365 nm UV light.

Photopatterning RGD on hydrogel surfaces

A custom synthesized benzophenone functionalized KGYSGRGDSPAS peptide sequence (BP-RGD) (Fig. S1†) is obtained from Biomatik USA. Hydrogel surfaces are photopatterned with freshly made solutions of 1 mg mL^{-1} BP-RGD in phosphate buffered saline (PBS, 137 mM NaCl). Prior to photopatterning, hydrogel samples are taken out of the gelation chamber and soaked in PBS (with release coverslip removed) to extract any small molecules remaining from gelation. A photomask is then attached to the bottom side of a standard 170 μm-thick coverslip, or a digital micromirror device (DMD) is used, and the focal plane is adjusted to be on the hydrogel surface. A volume of ~50 μL of 1 mg mL^{-1} BP-RGD solution is placed on the top of the coverslip, and the hydrogel is placed with its free surface downwards, in direct contact with the droplet. UV light (365 nm) is illuminated from the bottom through the photomask for ~30 min. Then hydrogel samples are then washed with ample PBS for 2 h to remove unreacted BP-RGD. To visualize RGD patterns, hydrogel samples are first soaked with 10 times concentrated PBS (1370 mM NaCl, adjusted to pH = 9 by adding sodium carbonate) (10× PBS) for 1 h, then incubated with freshly made fluorescein isothiocyanate (FITC)/10× PBS solution for another 8 h. Then hydrogel samples are washed again with ample amount of 10× PBS and then PBS to remove unreacted

FITC molecules. FITC labeled RGD patterns are imaged with 2.5× objective on a Zeiss inverted optical microscope (Zeiss Axiovert 200).

Cell culture

C2C12 myoblasts obtained from the American Type Culture Collection (ATCC) are expanded and frozen down. Cells are plated at equal density (3×10^5 cells per well) in 6-well culture plates that contained a glass slide coated with a hydrogel film and then with RGD. Cell cultures are maintained at 37 °C in a 5% CO_2 incubator in Dulbecco modified Eagle medium (DMEM) supplemented with 10% Fetal Bovine Serum (GM) and 1% penicillin and streptomycin. Cells used for all experiments are between passages 4–6. Cells are left to settle on RGD coated hydrogel substrates for 24 h and samples are rinsed once with fresh DMEM (with 10% FBS) at 37 °C prior to imaging using a 10× objective (Zeiss Axiovert 200) in differential interference contrast (DIC) and phase contrast mode and a Q-imaging camera (Retiga 2000R).

Image analysis

Changes in the size of cells are analyzed by Image J software. Line profiles are extracted at three different locations across a cell along both the *x*- and *y*-directions, and the corresponding cell dimension is determined by plotting pixel intensity profiles. The tensile strain is calculated by tracking changes in the cell dimensions averaged over the three measurements. When more than a single cell adheres to a pad, the overall change in the size of the cell cluster is considered instead of that of a single cell. An example of the image analysis process is shown in Fig. S5,† and the distribution of measured strains for cell clusters under plane strain condition is plotted in Fig. S6.†

Results and discussion

For a thin layer of hydrogel attached to a rigid substrate, swelling in an aqueous medium generates equibiaxial compression within the gel. Above some critical effective compressive strain, the hydrogel surface buckles into sharp self-contacting features, referred to as creases.[49] Our approach to cell stretching devices relies on several key features of creases. First, a crease is a localized, yet large amplitude, deformation of the surface. When a crease grows or shrinks in depth, nearby material points undergo in plane and vertical displacements that are both a sizable fraction of the film thickness, which is several μm for the gel films studied here. This means that rather large strains can be applied, with only slight motion of the cell with regards to the field-of-view and focal plane of an optical microscope, facilitating *in situ* observation. Second, topographic micro-patterns on the underlying rigid substrate can break the in-plane symmetry of stress on the gel surface and direct the spatial positioning of creases.[48] This allows us to precisely control the amount and type of strain applied to cells. Third, creases can be reversibly formed and annihilated on the surfaces of responsive gels by small variations in a variety of stimuli including temperature,[48] light intensity,[50] electric field strength,[51] solvent quality,[52] pH value and salt concentration,[53] providing a number of possible approaches to drive deformation of the gel surface. Here, we choose temperature as a convenient stimulus that allows for the application of large amounts of strain over a range that is not physiologically disruptive. However, we note that future designs can easily be envisioned that make use of any number of other stimuli. Finally, the critical swelling ratio for the onset of creasing is largely insensitive to elastic modulus (from ~100 Pa to MPa),[49] meaning that the method can potentially be implemented for substrates spanning the range of physiologically relevant stiffnesses, from that similar to brain, to that similar to bone-like tissue.[54] In our experiments, we employ hydrogels with a Young's modulus estimated as ~10 kPa from data in the literature on similar composition gels.[55] This is approximately an order of magnitude larger than the modulus reported for attached C2C12 myoblast cells of ~1 kPa,[56] suggesting that cell traction will lead to only modest deformation of the substrate.

However, to exploit creases for the controlled deformation of cultured cells, as shown schematically in Fig. 1, a challenge must first be overcome: namely, cultured cells must be induced to adhere to the gel surface in registry with the pattern of creases, such that folding and unfolding of the gel surface leads to application of the desired strain. While methods to pattern the surface chemistry of rigid substrates (plastic, glass, *etc.*) are widely used to spatially control cell attachment,[7,57] efforts to pattern biological ligands on soft gel substrates have so far been fairly limited.[58–64] These procedures usually require complicated multi-step processes,[59,61–64] and suffer other limitations that make them inappropriate for the soft, stimulus-responsive gels considered here: *i.e.*, they work only for gels with specific chemical functional

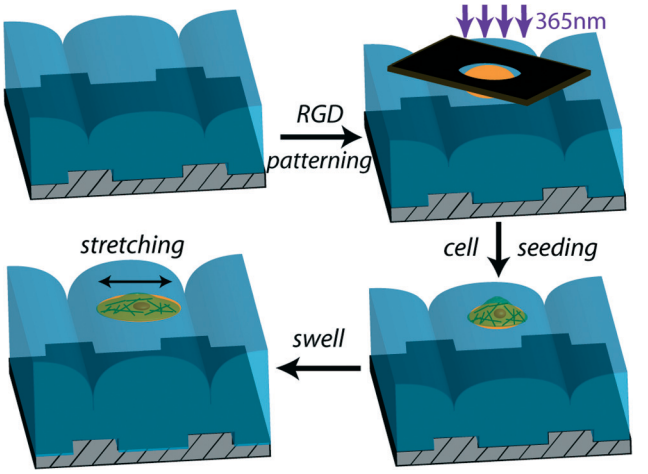

Fig. 1 Schematic illustration of the method for stretching cells with creased hydrogels. An RGD-containing peptide sequence is photopatterned onto the hydrogel surface between two neighboring creases, which are directed by topographic patterns on the underlying rigid substrate. Cells are subsequently seeded on the patterned surface and the swelling of the gel is modulated to stretch cells.

groups[60,64] or relatively high stiffness,[63] require the gel to be patterned in a non-solvated environment,[59,61] are only effective for gels with planar surfaces,[62] or alter the gel topography after functionalization.[58]

Here, we instead modify the approach of Hebert, *et al.*, for direct photo-patterning of peptides onto rigid substrates using benzophenone (BP) photo-chemistry.[57] Specifically, we used an end-functionalized peptide sequence BP-KGYSGRGDSPAS (BP-RGD) (Fig. S1†) capable of binding to integrin receptors in the cell membrane. In our approach, a poly(*N*-isopropylacrylamide)-copolymer hydrogel film supported on a glass substrate is immersed in phosphate buffered saline (PBS) containing BP-RGD. Illumination with UV light (365 nm) through a photomask or a digital micromirror device (DMD) leads to patterned attachment of the peptide sequence to the gel through the well-known photo-grafting chemistry of BP.[65] Confirmation of successful patterning was obtained by incubation with fluorescein isothiocyanate (FITC), which reacts selectively with the lysine (K) residue in the peptide, as shown in Fig. S1.† Specifically, the isothiocynate group of FITC reacts efficiently with the primary amine group of lysine (K) residue on the peptide sequence at pH 9 to form a thiourea bond.[66] To our knowledge, this simple approach provides the first one-step process that allows for patterning of biomolecules on both flat (Fig. S1.B†) and curved (Fig. S1.C†) gel surfaces, can be adapted to a wide variety of gel chemistries, and allows for patterning of low modulus gels with good fidelity. The fabrication of mechanically dynamic materials for cell culture has been a topic of recent interest[13,48,67] (as recently reviewed[68,69]), and we expect that the approach described here for one-step patterning of biological molecules onto dynamic surfaces with precise spatial control can have broader utility in this context beyond the specific goals of the current study.

To demonstrate this method of patterning hydrogel surfaces and determine the critical size of RGD features needed to support cell adhesion, we first fabricate a series of stripes and circular patterns with different dimensions, as summarized in Fig. 2. As controls, cells are also seeded on standard polystyrene (PS) culture dishes, hydrogels without RGD coating, and hydrogels uniformly coated with RGD. As shown in Fig. S2,† after 24 h, no cells adhere to the hydrogel surface without RGD coating, while cells adhere and spread on both the uniformly RGD coated hydrogels and the PS substrates. However, there is a lower cell density on the RGD coated gels compared to PS, presumably due to the relatively low density of photo-grafted RGD ligands compared to the level of protein adsorption on PS. For stripe patterns, a critical stripe width of ~60 μm is found for C2C12 cells to adhere in registry with surface patterns. As shown in Fig. 2A, when seeded on 60 μm stripes, cells line up "single file" along the stripe, and elongate along the stripe direction. Substantially larger stripes lead to multiple cells attached on a stripe cross section, while smaller stripes show poor cell adhesion and lack of alignment with the RGD pattern. For circular patterns, the critical pad size to achieve mostly single cells on pads is also found to be about 60 μm in diameter (Fig. 2B). For 40 μm pads, no cell adhesion is found for widely-spaced features, while a center-to-center spacing of 60 μm allow cells to bridge between two or three neighboring pads (Fig. 2C). These results are consistent with prior reports on the importance of RGD pattern geometry on cell attachment[7] and demonstrate that the current method is suitable for patterning adhesion at the single cell level. While 60 μm is found to be the minimum feature size for single cell adhesion, cells were still geometrically confined and do not spread well. In the following cell stretching experiments, slightly larger RGD pads are patterned.

To pattern the location of creases, we use a previously described approach[48] to form topographic features on the glass substrate, which break the in plane stress symmetry and direct a single crease to form above each raised feature. Fig. 3A shows cross-sectional images of a creased hydrogel from laser scanning fluorescence confocal microscopy (LSCM). At 37 °C, the hydrogel shows only a shallow crease, while the additional swelling of the gel upon reducing the temperature to 26 °C causes the crease to fold to a much greater depth. While the gel surface in the immediate vicinity of the crease is substantially curved, the region between two creases where cells will adhere (as denoted by the white line in Fig. 3A) is relatively flat. With the gel at room temperature (~22 °C), RGD is photo-patterned into an array of rectangular regions, each located between two neighboring creases. Dimensions

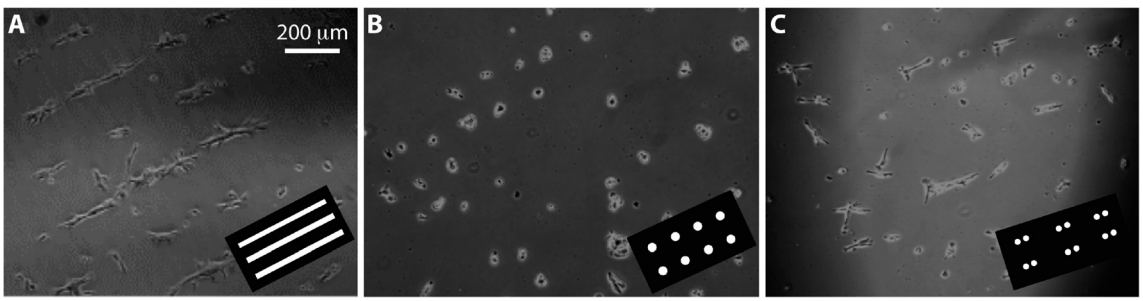

Fig. 2 Optical micrographs of C2C12 mouse myoblasts cultured on hydrogels patterned with (A) 60 μm wide stripes of RGD with 200 μm pitch, (B) 60 μm diameter circles, on which cells are primarily confined to a single dot, and (C) 40 μm diameter circles spaced by 60 μm, on which cells occasionally bridged between neighboring circles. Insets show schematic illustrations of the patterns on the photomasks used to photo-graft RGD (not to scale).

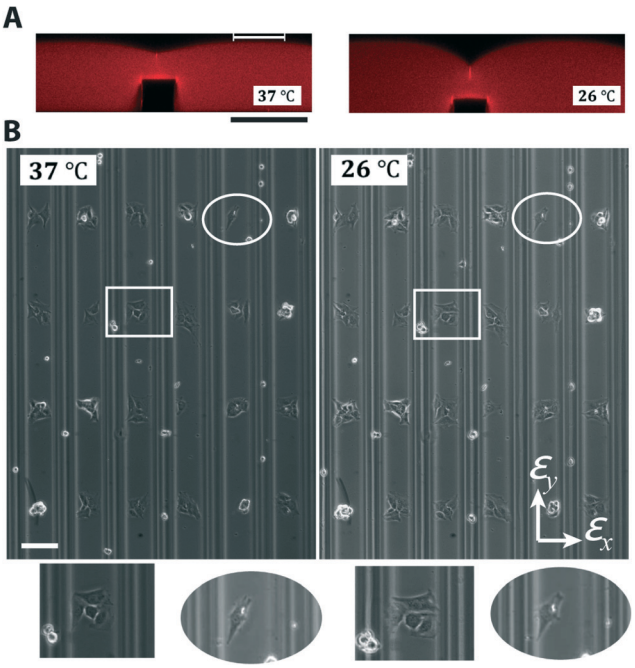

Fig. 3 Cells seeded between parallel creases are stretched under plane strain conditions. (A) A cross-sectional image from confocal fluorescence microscopy showing a shallow crease at 37 °C that grows into a deeper crease at 26 °C leading to tensile deformation of attached cells. The approximate region of cell adhesion is denoted by the white line. The depths of the cross-sectional images are limited by the working distance of the objective lens, thus only a small portion of the topographic feature on the substrate can be seen in the image at 26 °C. (B) Optical micrographs of cells seeded between neighboring parallel creases at 37 °C and subsequently placed under (plane-strain) tensile deformation of ε_x = 0.20 ± 0.03 and $\varepsilon_y \approx 0$ by reducing the temperature to 26 °C. Enlarged images corresponding to the rectangular and oval regions are shown below, clearly demonstrating the deformation of cells. The scale bars represent 100 μm.

of 70 μm along the crease direction and 90 μm in width are patterned at room temperature, which is reduced to roughly 70 × 70 μm at 37 °C where cells are seeded. These dimensions are chosen to be slightly larger than the critical size determined for single cell adhesion, to ensure good adhesion and spreading. For these dimensions, we find a distribution in the number of cells per pad (12% had 0 cells, 10% had 1 cell, 25% had 2 cells, 33% had 3 cells, and 20% had 4 or more cells), which can presumably be adjusted through fine-tuning of the pad size and cell seeding density.

Cells seeded at 37 °C adhere in good registry with the RGD pattern (Fig. 3B, left), and become stretched along the *x*-direction as the temperature is reduced to 26 °C (Fig. 3B, right). Due to the geometry of these creases as long parallel stripes, there is no displacement along the *y*-direction, thus, at 26 °C the cells experience a plane strain state of tension with ε_x = 0.20 ± 0.03 and $\varepsilon_y \approx 0$, as determined by measuring the change in the sizes of single cells or clusters from optical micrographs (Fig. S5–S6†). While the magnitude of this strain is above that cells usually experience *in vivo*, and previous studies have shown that strains above 0.20 can lead to cell death,[70,71] we choose this value to demonstrate the capability of the approach. Movie S1† shows how the size of a cell cluster changes as temperature is tuned over a time of ~30 min. As plotted in Fig. 4, the tensile strain increases up to 0.135 as the temperature is reduced from 37 to 26 °C and drops to nearly 0 as the temperature is raised back to 37 °C. Smaller strains can be achieved simply by varying temperature over smaller ranges.

Cells *in vivo* undergo many different kinds of mechanical deformation, thus the ability to vary not only the magnitude, but also the type, of applied strain is desirable. To achieve different strain states, we change the topographic patterns that template creases from parallel lines to ellipses of varying aspect ratio *a*/*b* (as shown in Fig. S3,† both stripes and an array of different elliptical patterns can be patterned on a single substrate). A circular pad of RGD (75 μm in diameter) directs adhesion of one or more cells at the center of each ellipse (roughly 35% of pads are occupied by 1 cell and 65% by 2–4 cells), as shown in Fig. 5. Reducing the temperature from 37 °C to 26 °C then applies a tensile strain with a degree of biaxiality dictated by the ellipse aspect ratio: (A) ε_x = 0.22, ε_y = 0.02 (*a*/*b* = 3/8), (B) ε_x = 0.15, ε_y = 0.08 (*a*/*b* = 1/2), (C) ε_x = 0.15, ε_y = 0.10 (*a*/*b* = 3/4), and (D) $\varepsilon_x = \varepsilon_y$ = 0.12 (equibiaxial, *a*/*b* = 1/1). Movie S2† shows the dynamic process of cell deformation for case (B). These results demonstrate that we can continuously tune the strain state from plane strain to equibiaxial stretching on a single substrate, which is an important step toward the development of a high throughput platform to study the effects of mechanical deformation on cells. For example, one central challenge in cellular mechanotransduction study is to identify how cells sense mechanical perturbations and convert them into biochemical signals. Achieving multiple strain states of cultured cells on a single substrate will enable high throughput study of the correlation between stress distribution and different signal pathways.

An important question to address is whether the apparent stretching of cells could reflect their response to the change

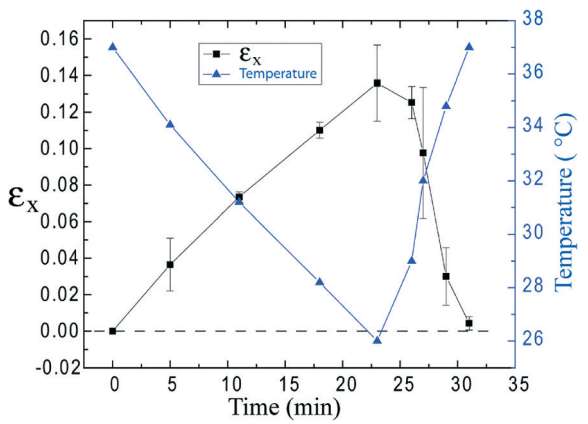

Fig. 4 The temperature (right axis) and tensile strain (left axis) experienced by the cell cluster shown in Movie 1 are plotted as a function of time during a cycle of cooling and heating, establishing excellent reversibility of cell stretching.

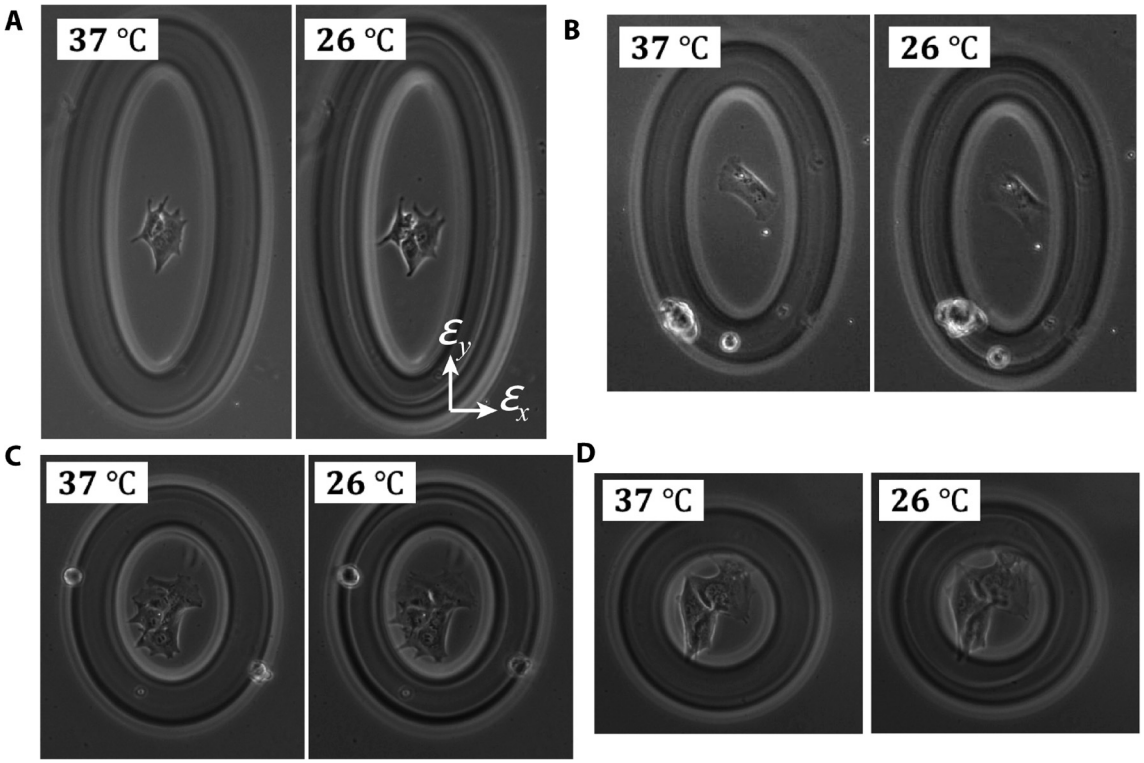

Fig. 5 Variations in the strain state are achieved through the use of templating ellipses with different aspect ratios. Cells are seeded at 37 °C and adhere to 75 μm diameter RGD patches at the center of each ellipse. Reducing the temperature to 26 °C causes the gel to further swell and applies a tensile strain to single, or in some cases several, cells under four different tensile states of increasing biaxiality: (A) ε_x = 0.22, ε_y = 0.02, (B) ε_x = 0.15, ε_y = 0.08, (C) ε_x = 0.15, ε_y = 0.10, and (D) ε_x = ε_y = 0.12 (equibiaxial).

in temperature in its own right. To address this point, a control experiment is performed on the flat unpatterned region of the same hydrogel surface coated with the same RGD peptide density. As shown in Movie S3,† over ~30 min, no measurable change in size occurs, indicating that the previous observations do indeed reflect mechanical deformations applied by the creased gel substrates. As shown in Fig. 6, the normalized size of cells or clusters, defined as the square root of the area divided by its initial value at 37 °C $\sqrt{A/A_0}$, is plotted as a function of time. We note that standard deviations as large as 0.03 are observed, presumably reflecting the active rearrangement of cytoskeleton and focal adhesions by individual cells. However, no significant change in average cell size is observed, confirming that temperature alone has minimal effects on cell dimensions over this range of temperatures (37 to 26 °C) and time frame (~30 min).

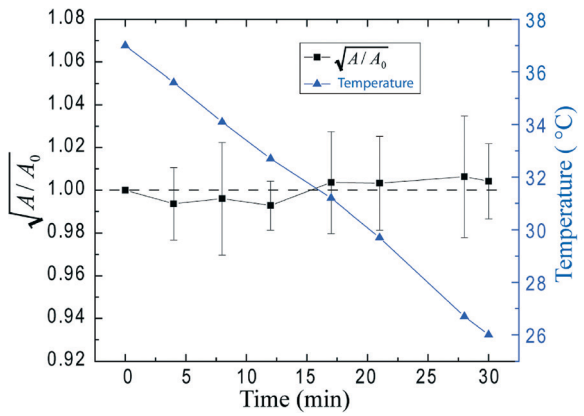

Fig. 6 The temperature (right axis) and normalized size of cells and clusters (left axis) is plotted as a function of time for cells on a flat, RGD-coated hydrogel substrate, revealing that the average cell size remains unchanged in the absence of creases.

However, although such temperature changes represent a relatively mild stimulus, the practical application of this approach would require care to separate any effects of temperature variation from those of mechanical stretch, and/or fine-tuning of the gel chemistry to substantially narrow the temperature variations required to achieve the desired strains. We note that thermally responsive gels have been developed that apply mechanical compression in 3D to cultured cells *via* volumetric changes occurring over a narrow temperature range,[6] which may offer a candidate material for future study. Additional drawbacks associated with the use of temperature as demonstrated here are the simultaneous global actuation of all folds, and the slow switching speeds. The former limitation could be addressed through the use of substrates patterned with micro-heaters,[72] or through photo-thermal temperature changes directed by patterns of light.[50] However, the latter limitation is more severe, due to the fundamental limit set by poroelastic swelling kinetics. Based on the gel thicknesses (H = 76 μm) used here and a previously reported value of the poroelastic diffusion constant[73] $D = 1.5 \times 10^{-11}$ m^2 s^{-1},

the intrinsic time scale for (one-dimensional) swelling is $\tau = H^2/(2D) \approx 200$ s. Attaining the high end of physiologically relevant strain rates of ~1 Hz, would therefore require a substantial decrease in H, perhaps coupled with modifications to the hydrogel structure to increase D.[74,75] Ultimately, the application of small electric potentials using micro-patterned electrodes, which yields quite rapid (~1–5 s) actuation of creases,[51] would be desirable if this method can be made compatible with cell culture.

Conclusions

In summary, we have demonstrated the use of hydrogel substrates with patterned creases and surface chemistries as a dynamic platform to apply tensile strain on cultured cells. Using temperature variation to drive deformation of the gel, the deformation of muscle cells with strain amplitudes up to 0.20 and strain states varying from plane strain to equibiaxial can be achieved. Compared to current, commercially available, cell stretching devices, the lack of macroscopic deformation greatly simplifies the process of conducting these experiments and making *in situ* observations of cell behavior. Further, it allows for the application of well-defined strains to either single cells or multi-cell clusters. With future developments to improve the switching speed, enable independent actuation of each crease, and minimize the effects of the driving stimulus itself on cell behavior, we anticipate this approach will provide a versatile tool for mechano-biological studies in contexts including stem cell engineering,[54] cancer biology, gene transfection[76] and kinesiological studies.[4,77]

Acknowledgements

The authors are indebted to Dr. Sangram S. Parelkar for help setting up our cell culture lab. Funding for this work was provided by the Center for Excellence in Apoptosis Research through a Pilot Award and the National Science Foundation through award DMR-1309331.

Notes and references

1 D. E. Ingber, *Ann. Med.*, 2003, **35**, 564–577.
2 H. Huang, R. D. Kamm and R. T. Lee, *Am. J. Physiol.*, 2004, **287**, C1–C11.
3 M. D. Buschmann, Y. A. Gluzband, A. J. Grodzinsky and E. B. Hunziker, *J. Cell Sci.*, 1995, **108**, 1497–1508.
4 B. L. Springer and P. M. Clarkson, *Med. Sci. Sports Exercise*, 2003, **35**, 1499–1502.
5 C. Ainsworth, *Nature*, 2008, **456**, 696–699.
6 B. Hashmi, L. D. Zarzar, T. Mammoto, A. Mammoto, A. Jiang, J. Aizenberg and D. E. Ingber, *Adv. Mater.*, 2014, **26**, 3253–3257.
7 C. S. Chen, M. Mrksich, S. Huang, G. M. Whitesides and D. E. Ingber, *Science*, 1997, **276**, 1425–1428.
8 V. Vogel and M. Sheetz, *Nat. Rev. Mol. Cell Biol.*, 2006, **7**, 265–275.
9 K. A. Kilian, B. Bugarija, B. T. Lahn and M. Mrksich, *Proc. Natl. Acad. Sci. U. S. A.*, 2010, **107**, 4872–4877.
10 C. J. Bettinger, R. Langer and J. T. Borenstein, *Angew. Chem., Int. Ed.*, 2009, **48**, 5406–5415.
11 K. Saha, A. J. Keung, E. F. Irwin, Y. Li, L. Little, D. V. Schaffer and K. E. Healy, *Biophys. J.*, 2008, **95**, 4426–4438.
12 D. E. Discher, P. Janmey and Y.-L. Wang, *Science*, 2005, **310**, 1139–1143.
13 K. A. Davis, K. A. Burke, P. T. Mather and J. H. Henderson, *Biomaterials*, 2011, **32**, 2285–2293.
14 P. Yang, R. M. Baker, J. H. Henderson and P. T. Mather, *Soft Matter*, 2013, **9**, 4705–4714.
15 M. Guvendiren and J. A. Burdick, *Biomaterials*, 2010, **31**, 6511–6518.
16 F. Greco, T. Fujie, L. Ricotti, S. Taccola, B. Mazzolai and V. Mattoli, *ACS Appl. Mater. Interfaces*, 2012, **5**, 573–584.
17 B. E. Sumpio and A. J. Banes, *J. Surg. Res.*, 1988, **44**, 696–701.
18 E. Wilson, Q. Mai, K. Sudhir, R. H. Weiss and H. E. Ives, *J. Cell Biol.*, 1993, **123**, 741–747.
19 D. E. Ingber, *FASEB J.*, 2006, **20**, 811–827.
20 A. W. Orr, B. P. Helmke, B. R. Blackman and M. A. Schwartz, *Dev. Cell*, 2006, **10**, 11–20.
21 D. A. Fletcher and R. D. Mullins, *Nature*, 2010, **463**, 485–492.
22 N. J. Sniadecki, A. Anguelouch, M. T. Yang, C. M. Lamb, Z. Liu, S. B. Kirschner, Y. Liu, D. H. Reich and C. S. Chen, *Proc. Natl. Acad. Sci. U. S. A.*, 2007, **104**, 14553–14558.
23 J. Fu, Y.-K. Wang, M. T. Yang, R. A. Desai, X. Yu, Z. Liu and C. S. Chen, *Nat. Methods*, 2010, **7**, 733–736.
24 W. R. Legant, C. K. Choi, J. S. Miller, L. Shao, L. Gao, E. Betzig and C. S. Chen, *Proc. Natl. Acad. Sci. U. S. A.*, 2013, **110**, 881–886.
25 M. Nikkhah, F. Edalat, S. Manoucheri and A. Khademhosseini, *Biomaterials*, 2012, **33**, 5230–5246.
26 L. Trichet, J. Le Digabel, R. J. Hawkins, S. R. K. Vedula, M. Gupta, C. Ribrault, P. Hersen, R. Voituriez and B. Ladoux, *Proc. Natl. Acad. Sci. U. S. A.*, 2012, **109**, 6933–6938.
27 Q. Tseng, I. Wang, E. Duchemin-Pelletier, A. Azioune, N. Carpi, J. Gao, O. Filhol, M. Piel, M. Théry and M. Balland, *Lab Chip*, 2011, **11**, 2231–2240.
28 R. D. Sochol, A. T. Higa, R. R. Janairo, S. Li and L. Lin, *Soft Matter*, 2011, **7**, 4606–4609.
29 M. A. Bucaro, Y. Vasquez, B. D. Hatton and J. Aizenberg, *ACS Nano*, 2012, **6**, 6222–6230.
30 T. D. Brown, *J. Biomech.*, 2000, **33**, 3–14.
31 Y. Kamotani, T. Bersano-Begey, N. Kato, Y.-C. Tung, D. Huh, J. W. Song and S. Takayama, *Biomaterials*, 2008, **29**, 2646–2655.
32 M. Dao, C. Lim and S. Suresh, *J. Mech. Phys. Solids*, 2003, **51**, 2259–2280.
33 G. Bao and S. Suresh, *Nat. Mater.*, 2003, **2**, 715–725.
34 R. M. Hochmuth, *J. Biomech.*, 2000, **33**, 15–22.
35 N. Wang, J. P. Butler and D. E. Ingber, *Science*, 1993, **260**, 1124–1127.
36 D. R. Overby, B. D. Matthews, E. Alsberg and D. E. Ingber, *Acta Biomater.*, 2005, **1**, 295–303.
37 D. L. Bader and M. M. Knight, *Med. Biol. Eng. Comput.*, 2008, **46**, 951–963.

38 S. A. Vanapalli, M. H. Duits and F. Mugele, *Biomicrofluidics*, 2009, **3**, 012006.
39 E. Zhou, X. Trepat, C. Park, G. Lenormand, M. Oliver, S. Mijailovich, C. Hardin, D. Weitz, J. Butler and J. Fredberg, *Proc. Natl. Acad. Sci. U. S. A.*, 2009, **106**, 10632–10637.
40 C. Moraes, J.-H. Chen, Y. Sun and C. A. Simmons, *Lab Chip*, 2010, **10**, 227–234.
41 D. Tremblay, S. Chagnon-Lessard, M. Mirzaei, A. E. Pelling and M. Godin, *Biotechnol. Lett.*, 2013, 1–9.
42 Y. Huang, N.-T. Nguyen, K. S. Lok, P. P. F. Lee, M. Su, M. Wu, L. Kocgozlu and B. Ladoux, *Nanomedicine*, 2013, **8**, 543–553.
43 J. M. Mann, R. H. Lam, S. Weng, Y. Sun and J. Fu, *Lab Chip*, 2012, **12**, 731–740.
44 D. Huh, B. D. Matthews, A. Mammoto, M. Montoya-Zavala, H. Y. Hsin and D. E. Ingber, *Science*, 2010, **328**, 1662–1668.
45 C. Simmons, J. Sim, P. Baechtold, A. Gonzalez, C. Chung, N. Borghi and B. Pruitt, *J. Micromech. Microeng.*, 2011, **21**, 054016.
46 S. Akbari and H. Shea, *J. Micromech. Microeng.*, 2012, **22**, 045020.
47 S. Akbari, S. Rosset and H. Shea, *Proc. SPIE*, 2012, **8340**, 83401R.
48 J. Kim, J. Yoon and R. C. Hayward, *Nat. Mater.*, 2009, **9**, 159–164.
49 V. Trujillo, J. Kim and R. C. Hayward, *Soft Matter*, 2008, **4**, 564–569.
50 J. Yoon, P. Bian, J. Kim, T. J. McCarthy and R. C. Hayward, *Angew. Chem.*, 2012, **124**, 7258–7261.
51 B. Xu and R. C. Hayward, *Adv. Mater.*, 2013, **25**, 5555–5559.
52 M. Guvendiren, J. A. Burdick and S. Yang, *Soft Matter*, 2010, **6**, 5795–5801.
53 L. Jin, D. Chen, R. C. Hayward and Z. Suo, *Soft Matter*, 2014, **10**, 303–311.
54 A. J. Engler, S. Sen, H. L. Sweeney and D. E. Discher, *Cell*, 2006, **126**, 677–689.
55 T. Yeung, P. C. Georges, L. A. Flanagan, B. Marg, M. Ortiz, M. Funaki, N. Zahir, W. Ming, V. Weaver and P. A. Janmey, *Cell Motil. Cytoskeleton*, 2005, **60**, 24–34.
56 E. Peeters, C. Oomens, C. Bouten, D. Bader and F. Baaijens, *J. Biomech.*, 2005, **38**, 1685–1693.
57 C. B. Herbert, T. L. McLernon, C. L. Hypolite, D. N. Adams, L. Pikus, C.-C. Huang, G. B. Fields, P. C. Letourneau, M. D. Distefano and W.-S. Hu, *Chem. Biol.*, 1997, **4**, 731–737.
58 M. S. Hahn, L. J. Taite, J. J. Moon, M. C. Rowland, K. A. Ruffino and J. L. West, *Biomaterials*, 2006, **27**, 2519–2524.
59 H. Takahashi, K. Emoto, M. Dubey, D. G. Castner and D. W. Grainger, *Adv. Funct. Mater.*, 2008, **18**, 2079–2088.
60 Z. Gu and Y. Tang, *Lab Chip*, 2010, **10**, 1946–1951.
61 X. Tang, M. Y. Ali and M. T. A. Saif, *Soft Matter*, 2012, **8**, 7197–7206.
62 N. Wang, E. Ostuni, G. M. Whitesides and D. E. Ingber, *Cell Motil. Cytoskeleton*, 2002, **52**, 97–106.
63 J. Lee, A. A. Abdeen, T. H. Huang and K. A. Kilian, *J. Mech. Behav. Biomed. Mater.*, 2014, **38**, 209–218.
64 C. A. Goubko, A. Basak, S. Majumdar and X. Cao, *J. Biomed. Mater. Res., Part A*, 2014, **102**, 381–391.
65 G. Dorman and G. D. Prestwich, *Biochemistry*, 1994, **33**, 5661–5673.
66 *Bioconjugate techniques*, ed. G. T. Hermanson, Academic press, London, 2013.
67 X. Zhu, K. L. Mills, P. R. Peters, J. H. Bahng, E. H. Liu, J. Shim, K. Naruse, M. E. Csete, M. Thouless and S. Takayama, *Nat. Mater.*, 2005, **4**, 403–406.
68 J. Kim and R. C. Hayward, *Trends Biotechnol.*, 2012, **30**, 426–439.
69 S. Kustra and C. J. Bettinger, *MRS Bull.*, 2012, **37**, 836–846.
70 E. Felder, M. Siebenbrunner, T. Busch, G. Fois, P. Miklavc, P. Walther and P. Dietl, *Am. J. Physiol.*, 2008, **295**, L849.
71 M. Sotoudeh, Y.-S. Li, N. Yajima, C.-C. Chang, T.-C. Tsou, Y. Wang, S. Usami, A. Ratcliffe, S. Chien and J. Y.-J. Shyy, *Am. J. Physiol.*, 2002, **282**, H1709–H1716.
72 X. Cheng, Y. Wang, Y. Hanein, K. F. Böhringer and B. D. Ratner, *J. Biomed. Mater. Res., Part A*, 2004, **70**, 159–168.
73 J. Yoon, S. Cai, Z. Suo and R. C. Hayward, *Soft Matter*, 2010, **6**, 6004–6012.
74 L.-W. Xia, R. Xie, X.-J. Ju, W. Wang, Q. Chen and L.-Y. Chu, *Nat. Commun.*, 2013, **4**, 2226.
75 T. Serizawa, K. Wakita and M. Akashi, *Macromolecules*, 2002, **35**, 10–12.
76 A. Sharei, J. Zoldan, A. Adamo, W. Y. Sim, N. Cho, E. Jackson, S. Mao, S. Schneider, M.-J. Han and A. Lytton-Jean, *Proc. Natl. Acad. Sci. U. S. A.*, 2013, **110**, 2082–2087.
77 S. A. Moeckel-Cole and P. M. Clarkson, *J. Strength Cond. Res.*, 2009, **23**, 1055–1059.